

See discussions, stats, and author profiles for this publication at: <https://www.researchgate.net/publication/263945525>

# Ag(I) Complexes Containing Flexible N,N'-Di(3-pyridyl)adipoamide Ligands: Syntheses, Structures, Ligand Conformations, and Crystal-to-Crystal Transformations

ARTICLE *in* CRYSTAL GROWTH & DESIGN · JANUARY 2012

Impact Factor: 4.89 · DOI: 10.1021/cg201417y

---

CITATIONS

35

READS

19

7 AUTHORS, INCLUDING:



Chun-wei Yeh

63 PUBLICATIONS 808 CITATIONS

[SEE PROFILE](#)



Tsun-Ren Chen

National Pingtung University of Education

20 PUBLICATIONS 259 CITATIONS

[SEE PROFILE](#)



Owen Wang

Chung Yuan Christian University

57 PUBLICATIONS 798 CITATIONS

[SEE PROFILE](#)

# Ag(I) Complexes Containing Flexible *N,N'*-Di(3-pyridyl)adipoamide Ligands: Syntheses, Structures, Ligand Conformations, and Crystal-to-Crystal Transformations

Pei-Chi Cheng,<sup>†</sup> Chun-Wei Yeh,<sup>†</sup> Wayne Hsu,<sup>†</sup> Tsun-Ren Chen,<sup>‡</sup> Hong-Wen Wang,<sup>†</sup> Jhy-Der Chen,<sup>\*,†</sup> and Ju-Chun Wang<sup>§</sup>

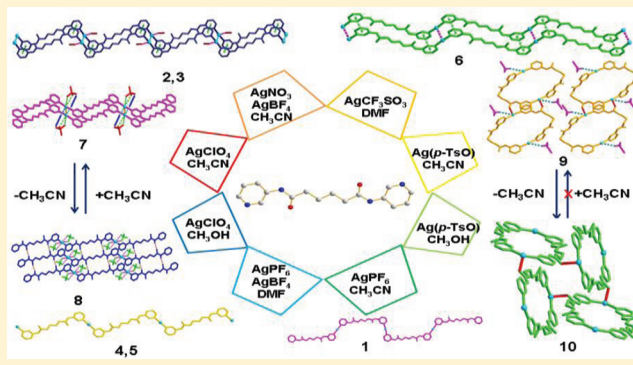
<sup>†</sup>Department of Chemistry, Chung-Yuan Christian University, Chung-Li, Taiwan, R.O.C.

<sup>‡</sup>Department of Chemical Biology, National Pingtung University of Education, PingTung, Taiwan, R.O.C.

<sup>§</sup>Department of Chemistry, Soochow University, Taipei, Taiwan, R.O.C.

## Supporting Information

**ABSTRACT:** The reactions of *N,N'*-di(3-pyridyl)adipoamide (**L**) with the corresponding silver(I) salts afforded the complexes  $\{[\text{Ag}(\text{L})](\text{PF}_6)_2 \cdot 2\text{CH}_3\text{CN}\}_{\infty}$ , **1**,  $\{[\text{Ag}(\text{L})](\text{BF}_4)_2 \cdot \text{CH}_3\text{CN}\}_{\infty}$ , **2**,  $\{[\text{Ag}(\text{L})](\text{NO}_3)_2 \cdot \text{CH}_3\text{CN}\}_{\infty}$ , **3**,  $\{[\text{Ag}(\text{L})](\text{PF}_6)_2 \cdot 4\text{DMF}\}_{\infty}$ , **4**,  $\{[\text{Ag}(\text{L})](\text{BF}_4)_2 \cdot 4\text{DMF}\}_{\infty}$ , **5**,  $\{[\text{Ag}(\text{L})](\text{CF}_3\text{SO}_3)_2 \cdot \text{DMF}\}_{\infty}$ , **6**,  $\{[\text{Ag}(\text{L})](\text{ClO}_4)_2 \cdot \text{CH}_3\text{CN}\}_{\infty}$ , **7**,  $\{[\text{Ag}(\text{L})](\text{ClO}_4)\}_{\infty}$ , **8**,  $[\text{Ag}_2(\text{L})_2]_2(p\text{-TsO})_2 \cdot 2\text{CH}_3\text{CN}$  (*p*-TsO = *p*-toluenesulfonate), **9**, and  $[\text{Ag}(\text{L})(p\text{-TsO})]_{\infty}$ , **10**. Complex **1** forms a one-dimensional (1D) concavo-convex chain, and complexes **2**, **3**, **6**, and **7** show 1D polymeric pairs of zigzag chains supported by the Ag--Ag and  $\pi$ -- $\pi$  interactions, whereas complexes **4**, **5**, and **8** adopt zigzag chains. Complex **9** forms a zero-dimensional (0D) dinuclear metallocycle, and complex **10** shows a two-dimensional (2D) pleated grid with a {4,8<sup>2</sup>} topology, respectively. The **L** ligands in these complexes adopt various ligand conformations, which are subjected to the changes of the counteranions and solvents, resulting in the different structural types. Reversible crystal-to-crystal transformation was observed in **7** and **8** upon removal and uptake of the acetonitrile molecules, while the process was irreversible in **9** and **10**, which is concomitant with changes in supramolecular structures, ligand conformations, and luminescent properties. The main driving forces for the structural transformations are the Ag--N and Ag--O interactions.



## INTRODUCTION

The rational design and synthesis of novel coordination polymers continue to be an active area of investigation because it expands the range of new complexes with preselected physical and chemical properties.<sup>1</sup> The range and variety of the self-assembling structures that can be constructed rely on the presence of suitable metal–ligand interactions and supramolecular contacts, that is, hydrogen bonding and other weak interactions.<sup>2</sup> Additionally, the structural types of the resulting coordination polymers are also affected by factors such as counterion,<sup>3</sup> metal-to-ligand ratio,<sup>4</sup> and solvent.<sup>5</sup> The networks of coordination polymers containing flexible bidentate ligands are less predictable due to the possible occurrence of supramolecular isomerism involving the adoption of different ligand conformations.<sup>6</sup> It has been shown that 1,2-bis(4-pyridyl)ethane can adopt either a *gauche* or *anti* geometry, and 1,3-bis(4-pyridyl)propane can exist in *anti-anti*, *gauche-anti*, and *gauche-gauche* conformations. However, the use of conformationally flexible ligands may provide unique opportunities to construct novel crystalline architectures with desirable characteristics.<sup>6f</sup> We have recently investigated the roles of ligand conformations

of the flexible dipyrindyl ligands bearing amide groups in the structural diversity,<sup>7</sup> and reported a series of one-dimensional (1D) silver(I) coordination polymers containing the flexible ligand *N,N'*-di(2-pyridyl)adipoamide (**L'**),<sup>7a</sup> involving the zigzag chains  $[\text{Ag}(\text{L}')(\text{NO}_3)]_{\infty}$ ,  $[\text{Ag}(\text{L}')(\text{PF}_6)]_{\infty}$ ,  $[\text{Ag}(\text{L}')(\text{BF}_4)_2 \cdot (\text{CH}_3\text{CN})(\text{H}_2\text{O})_{0.5}]_{\infty}$ , and  $[\text{Ag}(\text{L}')(\text{ClO}_4)(\text{CH}_3\text{CN})]_{\infty}$ , the helical chain  $[\text{Ag}(\text{L}')(\text{ClO}_4)(\text{H}_2\text{O})_{0.67}]_{\infty}$ , and the sinusoidal chain  $[\text{Ag}_2(\text{L}')_2\text{SO}_4]_{\infty}$ , which demonstrates an unusual co-existence of three ligand conformers in a coordination polymer. All the ligands in the zigzag and helical chains adopt the AAA trans conformation, and the three independent **L**'s in  $[\text{Ag}_2(\text{L}'_{2.5})\text{SO}_4]_{\infty}$  adopt GGG cis, AAA trans, and AGA cis conformations, respectively. These conformations also differ in the dihedral angle between the two pyridyl rings.

With this background information, we sought to investigate the role of ligand conformation of the isomeric *N,N'*-di(3-pyridyl)-adipoamide ligand in the structural diversity of silver(I)

Received: October 26, 2011

Revised: December 21, 2011

Published: January 4, 2012

coordination polymers. Herein, we report the syntheses, structures, and ligand conformations of  $\{[\text{Ag}(\text{L})](\text{PF}_6)\cdot2\text{CH}_3\text{CN}\}_{\infty}$ , **1**,  $\{[\text{Ag}(\text{L})](\text{BF}_4)\cdot\text{CH}_3\text{CN}\}_{\infty}$ , **2**,  $\{[\text{Ag}(\text{L})](\text{NO}_3)\cdot\text{CH}_3\text{CN}\}_{\infty}$ , **3**,  $\{[\text{Ag}(\text{L})](\text{PF}_6)\cdot4\text{DMF}\}_{\infty}$ , **4**,  $\{[\text{Ag}(\text{L})](\text{BF}_4)\cdot4\text{DMF}\}_{\infty}$ , **5**,  $\{[\text{Ag}(\text{L})](\text{CF}_3\text{SO}_3)\cdot\text{DMF}\}_{\infty}$ , **6**,  $\{[\text{Ag}(\text{L})](\text{ClO}_4)\cdot\text{CH}_3\text{CN}\}_{\infty}$ , **7**,  $\{[\text{Ag}(\text{L})](\text{ClO}_4)\}_{\infty}$ , **8**,  $[\text{Ag}_2(\text{L})_2](p\text{-TsO})_2\cdot2\text{CH}_3\text{CN}$  ( $p\text{-TsO}$  =  $p$ -toluenesulfonate), **9**, and  $[\text{Ag}(\text{L})(p\text{-TsO})]_{\infty}$ , **10**, which form zero-dimensional (0D) metallocycle, 1D coordination polymers involving concavo-convex chains, polymeric pairs of zigzag chains supported by the Ag--Ag and  $\pi-\pi$  interactions and zigzag chains, and a two-dimensional (2D) pleated grid. Complexes **7–10** form two pairs of Ag(I) complexes showing crystal-to-crystal transformations driven by the removal of the acetonitrile molecules. The transformation for the 1D zigzag chains **7** and **8** is reversible, while the process from the 0D dinuclear metallocycle **9** to the 2D pleated grid **10** is irreversible. These transformations were accompanied by changes in supramolecular structures, ligand conformations, and luminescent properties.

## EXPERIMENTAL SECTION

**General Procedures.** Elemental analyses were performed on a HERAEUS VaruoEL analyzer. IR spectra (KBr disk) were recorded on a Jasco FT/IR-460 plus spectrometer. Powder X-ray diffraction (PXRD) measurements were performed on a PANalytical PW3040/60 X'pert Pro diffractometer. Thermogravimetry analysis was carried out on a Mettler-Toledo STAR<sup>e</sup> analyzer. Emission spectra were determined in the solid state at room temperature using a Hitachi F-4500 spectrometer.

**Materials.** The reagents  $\text{AgPF}_6$ ,  $\text{AgBF}_4$ ,  $\text{AgNO}_3$ ,  $\text{AgCF}_3\text{SO}_3$ ,  $\text{AgClO}_4$ , and  $\text{Ag}(p\text{-TsO})$  were purchased from Aldrich Chemical Co. The ligand *N,N'*-di(3-pyridyl)adipoamide was prepared according to published procedures.<sup>7c</sup> Caution: Perchlorate salts are dangerous (especially if they are dry) and should be handled with care.

**Synthesis of  $\{[\text{Ag}(\text{L})](\text{PF}_6)\cdot2\text{CH}_3\text{CN}\}_{\infty}$  (1).**  $\text{L}$  (0.30 g, 1.0 mmol) was placed in a flask containing 15 mL of  $\text{CH}_3\text{CN}$  and  $\text{AgPF}_6$  (0.25 g, 1.0 mmol) was added. The mixture was then heated at reflux for 3 h to afford a yellow solution with some white solid. The solution was filtered and diethyl ether was added to induce precipitation. The precipitate was filtered, washed with diethyl ether, and then dried under a vacuum to give a white product. Yield: 0.44 g (69%, based on Ag). Anal. Calcd. for  $\text{C}_{20}\text{H}_{24}\text{AgF}_6\text{N}_6\text{O}_2\text{P}$  (MW = 633.29): C, 37.93; H, 3.82; N, 13.27%. Found: C, 38.43; H, 4.16; N, 12.54%. IR (KBr disk,  $\text{cm}^{-1}$ ): 3108(br), 1684(s), 1607(m), 1587(m), 1532(s), 1486(s), 1418(m), 1296(m), 835(s), 699(w). Colorless crystals were obtained by slow diffusion of diethyl ether into a  $\text{CH}_3\text{CN}$  solution of the compound for several weeks.

**Synthesis of  $\{[\text{Ag}(\text{L})](\text{BF}_4)\cdot\text{CH}_3\text{CN}\}_{\infty}$  (2).** Prepared as described for **1**, except that  $\text{AgBF}_4$  (0.19 g, 1.0 mmol) was used. Yield: 0.42 g (79%, based on Ag). Anal. Calcd for  $\text{C}_{18}\text{H}_{21}\text{AgBF}_4\text{N}_5\text{O}_2$  (MW = 534.08): C, 40.48; H, 3.96; N, 13.11%. Found: C, 40.61; H, 4.14; N, 13.37%. IR (KBr disk,  $\text{cm}^{-1}$ ): 3102(br), 1691(s), 1610(w), 1582(m), 1550(s), 1487(m), 1463(w), 1423(s), 1287(m), 1036(br), 808(m), 702(w).

**Synthesis of  $\{[\text{Ag}(\text{L})](\text{NO}_3)\cdot\text{CH}_3\text{CN}\}_{\infty}$  (3).** Prepared as described for **1**, except that  $\text{AgNO}_3$  (0.17 g, 1.0 mmol) was used. Yield: 0.35 g (69%, based on Ag). Anal. Calcd for  $\text{C}_{18}\text{H}_{21}\text{AgN}_6\text{O}_5$  (MW = 509.28): C, 42.45; H, 4.16; N, 16.50%. Found: C, 41.73; H, 3.79; N, 15.71%. IR (KBr disk,  $\text{cm}^{-1}$ ): 3102(br), 1691(m), 1668(w), 1611(w), 1583(s), 1551(s), 1480(m), 1463(w), 1423(s), 1383(s), 1286(m), 692(w).

**Synthesis of  $\{[\text{Ag}(\text{L})](\text{PF}_6)\cdot4\text{DMF}\}_{\infty}$  (4).**  $\text{L}$  (0.30 g, 1.0 mmol) was placed in a flask containing 15 mL of DMF, and  $\text{AgPF}_6$  (0.25 g, 1.0 mmol) was added. The mixture was heated at reflux for 3 h to afford a yellow solution with some white solid. The solution was filtered and diethyl ether was added to induce precipitation. The precipitate was filtered, washed with diethyl ether, and then dried under a vacuum to give a white product. Colorless crystals were obtained by slow

diffusion of diethyl ether into a DMF solution of the compound for several weeks. Yield: 0.39 g (46%, based on Ag). Anal. Calcd for  $\text{C}_{28}\text{H}_{46}\text{AgF}_6\text{N}_8\text{O}_6\text{P}$  (MW = 843.57.): C, 39.87; H, 5.50; N, 13.28%. Found: C, 39.09; H, 4.80; N, 12.57%. IR (KBr disk,  $\text{cm}^{-1}$ ): 3101(br), 1689(s), 1609(w), 1582(m), 1551(m), 1475(m), 1463(w), 1423(s), 1287(m), 842(s), 701(w).

**Synthesis of  $\{[\text{Ag}(\text{L})](\text{BF}_4)\cdot4\text{DMF}\}_{\infty}$  (5).** Prepared as described for **4**, except that  $\text{AgBF}_4$  (0.19 g, 1.0 mmol) was used. Yield: 0.36 g (46%, based on Ag). Anal. Calcd for  $\text{C}_{28}\text{H}_{46}\text{AgBF}_4\text{N}_8\text{O}_6$  (MW = 785.41): C, 42.82; H, 5.90; N, 14.27%. Found: C, 42.11; H, 5.18; N, 13.57%. IR (KBr disk,  $\text{cm}^{-1}$ ): 3106(br), 1687(s), 1654(s), 1582(m), 1551(m), 1523(m), 1475(m), 1422(s), 1285(m), 1034(br), 808(w), 701(w).

**Synthesis of  $\{[\text{Ag}(\text{L})](\text{CF}_3\text{SO}_3)\cdot\text{DMF}\}_{\infty}$  (6).** Prepared as described for **4** except that  $\text{AgCF}_3\text{SO}_3$  (0.26 g, 1.0 mmol) was used. Yield: 0.39 g (62%, based on Ag). Anal. Calcd for  $\text{C}_{20}\text{H}_{25}\text{AgF}_3\text{N}_5\text{O}_6\text{S}$  (MW = 628.38): C, 38.23; H, 4.01; N, 11.15%. Found: C, 38.32; H, 3.88; N, 11.40%. IR (KBr disk,  $\text{cm}^{-1}$ ): 3125(br), 1688(m), 1654(s), 1585(m), 1549(m), 1479(w), 1424(s), 1326(w), 1286(s), 1251(s), 1161(s), 1027(m), 694(w), 635(m).

**Synthesis of  $\{[\text{Ag}(\text{L})](\text{ClO}_4)\cdot\text{CH}_3\text{CN}\}_{\infty}$  (7).**  $\text{L}$  (0.30 g, 1.0 mmol) was placed in a flask containing 15 mL of  $\text{CH}_3\text{CN}$  and  $\text{AgClO}_4$  (0.21 g, 1.0 mmol) was then added. The mixture was heated at reflux for 3 h to afford a yellow solution with some white solid. The solution was filtered and diethyl ether was added to induce precipitation. The precipitate was filtered, washed with diethyl ether, and then dried under a vacuum to give a white product. Colorless crystals were obtained by slow diffusion of diethyl ether into a  $\text{CH}_3\text{CN}$  solution of the compound for several weeks. Yield: 0.41 g (75%, based on Ag). Anal. Calcd for  $\text{C}_{18}\text{H}_{21}\text{AgClN}_5\text{O}_6$  (MW = 546.72): C, 39.54; H, 3.87; N, 12.81%. Found: C, 39.50; H, 4.50; N, 12.92%. IR ( $\text{cm}^{-1}$ ): 3326(w), 3068(br), 1689(s), 1603(m), 1582(m), 1551(s), 1476(m), 1461(w), 1423(s), 808(m).

**Synthesis of  $\{[\text{Ag}(\text{L})](\text{ClO}_4)\}_{\infty}$  (8).** **8** was prepared as described for **7**, except that  $\text{CH}_3\text{OH}$  was used as the solvent. Yield: 0.34 g (67%, based on Ag). Anal. Calcd for  $\text{C}_{16}\text{H}_{18}\text{AgClN}_4\text{O}_6$  (MW = 505.66): C, 38.00; H, 3.59; N, 11.08%. Found: C, 38.13; H, 3.64; N, 11.47%. IR ( $\text{cm}^{-1}$ ): 3315(w), 3068(br), 1665(s), 1603(m), 1582(m), 1530(s), 1476(m), 1461(w), 1421(s), 818(m). Colorless crystals were obtained by slow diffusion of diethyl ether into a  $\text{CH}_3\text{OH}$  solution of the compound for several weeks.

**Synthesis of  $[\text{Ag}_2(\text{L})_2](p\text{-TsO})_2\cdot2\text{CH}_3\text{CN}$  (9).** **9** was prepared as described for **7**, except that  $\text{Ag}(p\text{-TsO})$  (0.28 g, 1.0 mmol) was used. Yield: 0.44 g (71%, based on Ag). Anal. Calcd for  $\text{C}_{50}\text{H}_{56}\text{Ag}_2\text{N}_{10}\text{O}_{10}\text{S}_2$  (MW = 1236.91): C, 48.55; H, 4.56; N, 11.32%. Found: C, 48.16; H, 4.70; N, 10.99%. IR ( $\text{cm}^{-1}$ ): 3556(w), 3104(br), 1689(s), 1611(m), 1581(m), 1551(s), 1475(m), 1463(w), 1424(s), 808(m).

**Synthesis of  $[\text{Ag}(\text{L})(p\text{-TsO})]_{\infty}$  (10).** **10** was prepared as described for **9**, except that  $\text{CH}_3\text{OH}$  was used as solvent. Yield: 0.45 g (78%, based on Ag). Anal. Calcd for  $\text{C}_{23}\text{H}_{25}\text{AgN}_4\text{O}_5\text{S}$  (MW = 577.40): C, 47.84; H, 4.36; N, 9.70%. Found: C, 47.62; H, 4.60; N, 9.82%. IR ( $\text{cm}^{-1}$ ): 3254(w), 3060(br), 1689(s), 1605(m), 1583(m), 1547(s), 1483(m), 1463(w), 1422(s), 806(m).

**Thermal Gravimetric Analyses for 1–10.** The samples were heated in nitrogen gas at a pressure of 1 atm with a heating rate of  $10\text{ }^{\circ}\text{C min}^{-1}$  and finished at  $900\text{ }^{\circ}\text{C}$ . Complexes **1** and **4** are stable at  $40\text{ }^{\circ}\text{C}$ . A total weight loss of 12.5% for **1** and 34.2% for **4** occurred in the range  $40\text{--}100\text{ }^{\circ}\text{C}$  and  $40\text{--}160\text{ }^{\circ}\text{C}$ , respectively, presumably due to the removal of the cocrystallized  $\text{CH}_3\text{CN}$  and DMF (calcd 13.0% for **1** and 34.7% for **4**), respectively. The weight loss of 69.5 for **1** and 52.3% for **4**, occurring at  $100\text{--}900\text{ }^{\circ}\text{C}$  and  $160\text{--}900\text{ }^{\circ}\text{C}$ , can be ascribed to the decomposition of the **L** ligands and the  $\text{PF}_6^-$  anions (calcd 70.0% for **1** and 52.6% for **4**).

Complex **2** is stable up to  $40\text{ }^{\circ}\text{C}$  and complex **5** is stable up to  $120\text{ }^{\circ}\text{C}$ , respectively. A total weight loss of 7.6% for **2** and 37.7% for **5** occurred in the range  $40\text{--}50\text{ }^{\circ}\text{C}$  and  $120\text{--}170\text{ }^{\circ}\text{C}$ , presumably due to the removal of the cocrystallized  $\text{CH}_3\text{CN}$  and DMF (calcd 7.7% for **2** and 37.2% for **5**). The weight loss of 71.6% and 48.5% for **2** and **5**, respectively, occurring in the temperature  $50\text{--}900$  and  $170\text{--}900\text{ }^{\circ}\text{C}$ , can be ascribed to the decomposition of the **L** ligands and the  $\text{BF}_4^-$  anions (calcd 72.1% for **2** and 49.0% for **5**).

Complex **3** is stable at 40 °C. A total weight loss of 8.3% occurred in the range 40–150 °C, presumably due to the removal of the cocrystallized CH<sub>3</sub>CN (calcd 8.1%). The weight loss of 70.6% occurring in the range 150–900 °C can be ascribed to the decomposition of the L ligands and the NO<sub>3</sub><sup>-</sup> anions (calcd 70.8%). Complex **6** is stable at 90 °C. A total weight loss of 11.4% occurred in the range 90–200 °C, presumably due to the removal of the cocrystallized DMF (calcd 11.6%). The weight loss of 71.1% occurring in the range 200–900 °C can be ascribed to the decomposition of the L ligands and the CF<sub>3</sub>SO<sub>3</sub><sup>-</sup> anions (calcd 71.2%).

Complex **7** is stable up to 130 °C. A total weight loss of 7.3% occurred in the range 130–200 °C, presumably due to the removal of the cocrystallized CH<sub>3</sub>CN (calcd 7.5%). The solid residue formed at around 200 °C is suggested to be the desolvation product. The weight loss of 72.5 and 78.3% for **7** and **8**, respectively, at the range 200–900 °C can be ascribed to the decomposition of the L ligands and the ClO<sub>4</sub><sup>-</sup> anions (calcd 72.8% for **7** and 78.7% for **8**).

Complex **9** is stable up to 110 °C. A total weight loss of 6.2% occurred in the range 110–140 °C, which can be ascribed to the removal of the cocrystallized CH<sub>3</sub>CN (calcd 6.6%). The solid residue formed at around 140 °C is suggested to be the desolvation product. The weight loss of 47.9 and 51.5% for **9** and **10**, respectively, occurring in the temperature 140–425 °C, is due to the decomposition of the L ligands (calcd 48.2% for **9** and 51.7% for **10**). Another weight loss of 27.5 and 29.2%, for **9** and **10**, respectively, at the range 425–900 °C is due to the decomposition of the anions (calcd 27.7% for **9** and 29.6% for **10**).

**X-ray Crystallography.** The diffraction data of complexes **1**–**10** were collected at 22 °C on a Bruker AXS P4 diffractometer (**2**, **3**, **8**, and **10**), a Bruker AXS KAPPA APEX II diffractometer (**1** and **6**), or a Bruker AXS SMART-1000 diffractometer (**4**, **5**, **7**, and **9**), which were equipped with a graphite-monochromated Mo K $\alpha$  ( $\lambda_{\alpha} = 0.71073 \text{ \AA}$ ) radiation. Data reduction was carried by standard methods with the use of well-established computational procedures.<sup>8</sup> The structure factors were obtained after Lorentz and polarization correction. An empirical absorption correction based on a series of  $\psi$ -scans was applied to the data for complexes **2**, **3**, **8**, and **10**, while the empirical absorption correction based on “multi-scan” was applied to the data for the other complexes. The positions of some of the heavier atoms, including the silver atom, were located by the direct method. The remaining atoms were found in a series of alternating difference Fourier maps and least-squares refinements.<sup>9</sup> Basic information pertaining to crystal parameters and structure refinement is summarized in Table 1. Selected bond distances and angles are listed in Table 2. The ORTEP diagrams showing the asymmetric units of **1**–**6** are provided as Supporting Information in Figures S1–S6.

## ■ RESULTS AND DISCUSSION

**Structures of {[Ag(L)](PF<sub>6</sub>)·2CH<sub>3</sub>CN}<sub>∞</sub> (**1**), {[Ag(L)](BF<sub>4</sub>)·CH<sub>3</sub>CN}<sub>∞</sub> (**2**), and {[Ag(L)](NO<sub>3</sub>)·CH<sub>3</sub>CN}<sub>∞</sub> (**3**).** The crystals of complex **1** conform to the space group  $P\bar{1}$  and those of **2** and **3** conform to the space group  $P2_1/c$ , respectively. Figure 1a,b depicts the structures of their cations. The silver(I) ions in each complex are bridged by two L ligands through the pyridyl nitrogen atoms in approximately linear geometries, resulting in the 1D concavo-convex chain for **1** and 1D zigzag chains for **2** and **3**, respectively. The 1D zigzag chains in **2** and **3** are supported by the Ag–Ag [3.218(2) Å for **2** and 3.391(1) Å for **3**] and  $\pi$ – $\pi$  [3.608(1) Å for **2** and 3.593(1) Å for **3**] interactions to form 1D polymeric pairs. The structural differences in **1**–**3** exhibit the influence of the counteranions on the structural diversity of Ag(I) complexes containing the L ligands, and may mainly be attributed to the differences in the shapes and coordination abilities of the anions. In **1**, the uncoordinated PF<sub>6</sub><sup>-</sup> anions are located between the 1D concavo-convex chains and interacted with them through a series of C–H---F [H---F = 2.428(3)–2.603(3) Å,  $\angle$ C–H---F = 129.3(2)–152.1(2) $^{\circ}$ ] hydrogen bonds, whereas the BF<sub>4</sub><sup>-</sup> anions

in **2** bridge the zigzag chains through C–H---F [H---F = 2.55(6) and 2.62(6) Å,  $\angle$ C–H---F = 133.7(5) and 139.2(4) $^{\circ}$ ] hydrogen bonds and the NO<sub>3</sub><sup>-</sup> anions in **3** interact with the silver(I) metal centers through Ag---O [2.7801(3) Å] interactions. The CH<sub>3</sub>CN molecules in **1**–**3** interact with the silver(I) metal centers through Ag---N interactions [Ag---N = 2.745(4) and 2.805(4) Å in **1**, 2.66(4) Å in **2**, and 2.683(1) in **3**].

**Structures of {[Ag(L)](PF<sub>6</sub>)·4DMF}<sub>∞</sub> (**4**), {[Ag(L)](BF<sub>4</sub>)·4DMF}<sub>∞</sub> (**5**) and {[Ag(L)](CF<sub>3</sub>SO<sub>3</sub>)·DMF}<sub>∞</sub> (**6**).** The crystals of complexes **4** and **5** conform to the space group  $P2_1/c$  and those of **6** conform to the space group  $P\bar{1}$ , respectively. Figure 1c,d depicts the structures of their cations. The silver(I) ions in each complex are bridged by the L ligands through the pyridyl nitrogen atom in approximately linear geometries, forming the zigzag chains for all three complexes. The 1D zigzag chains of **6** are also supported by the Ag–Ag [3.119(1) Å] and  $\pi$ – $\pi$  [3.506(1) Å and 3.551(1) Å] interactions to form 1D polymeric pairs. While the DMF molecules in **4**–**6** interact with the silver(I) metal centers through Ag---O [2.712(3) Å in **4**; 2.952(3) and 3.001(4) Å in **5**; 2.662(3) and 2.974(3) Å in **6**] interactions, the PF<sub>6</sub><sup>-</sup> and BF<sub>4</sub><sup>-</sup> anions interact with the chains through C–H---F [H---F = 2.560(5) and 2.618(5) Å,  $\angle$ C–H---F = 132.2(3) and 148.1(3) $^{\circ}$  in **4**; H---F = 2.503(4) and 2.617(3) Å,  $\angle$ C–H---F = 149.4(3) and 122.9(3) $^{\circ}$  in **5**] hydrogen bonds and the CF<sub>3</sub>SO<sub>3</sub><sup>-</sup> anion bridge adjacent chains through a series of N–H---O [H---O = 2.260(5)–2.589(7) Å,  $\angle$ N–H---O = 145.24(24)–148.45(22) $^{\circ}$ ] and C–H---O [H---O = 2.501(7)–2.707(7) Å,  $\angle$ C–H---O = 145.6(3)–147.5(3) $^{\circ}$ ] hydrogen bonds.

**Structures of {[Ag(L)](ClO<sub>4</sub>)·CH<sub>3</sub>CN}<sub>∞</sub> (**7**) and {[Ag(L)](ClO<sub>4</sub>)<sub>2</sub>}<sub>∞</sub> (**8**).** Crystals of complexes **7** and **8** conform to the space groups  $P2_1/c$  and  $C2/c$ , respectively, and Figure 2a,b depicts the coordination environments of their silver(I) centers. In both complexes, each silver(I) metal center is coordinated by two pyridyl nitrogen atoms with the N–Ag–N angle of 172.9(1) $^{\circ}$  for **7** and 180.0(1) $^{\circ}$  for **8**, respectively. Figure 2c shows the differences in the supramolecular structures between **7** and **8**. The ClO<sub>4</sub><sup>-</sup> anions in each complex interact with silver(I) centers through Ag---O [2.823(2)–3.231(1) Å in **7** and 2.961(2)–2.977(3) Å in **8**] interactions. The zigzag chains of **7** are supported by the Ag–Ag [3.140(3) Å] and  $\pi$ – $\pi$  [3.544(2) Å] interactions to form 1D polymeric pairs, while those of **8** are interlinked through N–H---O [H---O = 2.115(2) Å;  $\angle$ N–H---O = 160.1(1) $^{\circ}$ ] hydrogen bonds to form 2D pleated nets. In **7**, the acetonitrile molecules interact with the silver(I) center through the Ag---N [2.590(3) Å] interactions. Removal of the acetonitrile molecules in **7** thus results in a significantly different supramolecular structure in **8**. It is noted that attempts to grow crystals for X-ray diffraction studies by slow diffusion of diethyl ether into the CH<sub>3</sub>OH solutions of the compounds **1**–**6** were not successful.

**Structures of [Ag<sub>2</sub>(L)<sub>2</sub>](p-TsO)<sub>2</sub>·2CH<sub>3</sub>CN (**9**) and [Ag(L)(p-TsO)]<sub>∞</sub> (**10**).** Crystals of complexes **9** and **10** conform to the space groups  $P\bar{1}$  and  $P2_1/c$ , respectively, and Figure 3a,b depicts the coordination environments of their silver(I) centers. Complex **9** forms a dinuclear metallacycle in which each Ag(I) atom is coordinated by two pyridyl nitrogen atoms from two L ligands, resulting in a distorted linear geometry [N–Ag–N = 164.15(7) $^{\circ}$ ]. The 30-membered {Ag<sub>2</sub>N<sub>8</sub>C<sub>20</sub>} ring has the ring size of 9.12 × 15.89 Å<sup>2</sup>. The p-TsO anions interact with the cations through Ag---O [2.711(2)–2.974(1) Å] interactions, and the acetonitrile molecules interact with the anions and the cations through C–H---O [H---O = 2.482(2) Å;  $\angle$ C–H–O = 145.6(2) $^{\circ}$ ] hydrogen

Table 1. Crystal Data for Complexes 1–10

| compound   | 1  | 2   | 3   | 4  | 5   |
|--|--|---|---|--|---|
| formula  | C <sub>20</sub> H <sub>24</sub> AgF <sub>6</sub> N <sub>6</sub> O <sub>2</sub> P | C <sub>18</sub> H <sub>21</sub> AgBF <sub>4</sub> N <sub>5</sub> O <sub>2</sub> | C <sub>18</sub> H <sub>21</sub> AgN <sub>6</sub> O <sub>5</sub>   | C <sub>28</sub> H <sub>46</sub> AgF <sub>6</sub> N <sub>8</sub> O <sub>6</sub> P               | C <sub>28</sub> H <sub>46</sub> AgBF <sub>4</sub> N <sub>8</sub> O <sub>6</sub> |
| fw   | 633.29   | 534.08  | 509.28  | 843.57   | 785.41  |
| crystal system   | triclinic  | monoclinic  | monoclinic  | monoclinic   | monoclinic  |
| space group  | P $\bar{1}$  | P <sub>2</sub> <sub>1</sub> /c  | P <sub>2</sub> <sub>1</sub> /c                                    | P <sub>2</sub> <sub>1</sub> /c   | P <sub>2</sub> <sub>1</sub> /c  |
| <i>a</i> , Å   | 9.7697(4)  | 11.415(5)   | 11.1897(18)   | 8.4346(4)  | 8.8012(2)   |
| <i>b</i> , Å   | 14.8807(6)   | 13.1961(18)   | 13.3167(16)   | 31.3587(13)  | 29.8243(9)  |
| <i>c</i> , Å   | 18.5813(8)   | 13.949(3)   | 13.6307(19)   | 14.0692(6)   | 13.6026(4)  |
| $\alpha$ , °   | 90.600(2)  | 90  | 90  | 90   | 90  |
| $\beta$ , °  | 102.707(2)   | 90.15(3)  | 92.044(11)  | 98.772(4)  | 99.818(3)   |
| $\gamma$ , °   | 104.455(2)   | 90  | 90  | 90   | 90  |
| <i>V</i> , Å <sup>3</sup>  | 2545.65(18)  | 2101.1(11)  | 2029.8(5)   | 3677.7(3)  | 3518.25(17)   |
| <i>Z</i>   | 4  | 4   | 4   | 4  | 4   |
| <i>D</i> <sub>calcd</sub> , g/cm <sup>3</sup>                      | 1.652  | 1.688   | 1.667   | 1.524  | 1.483   |
| <i>F</i> (000)   | 1272   | 1072  | 1032  | 1736   | 1624  |
| $\mu$ (Mo K <sub>α</sub> ), mm <sup>-1</sup>                       | 0.928  | 1.020   | 1.037   | 0.672  | 0.645   |
| range(2θ) for data collection, deg                                 | 2.26 ≤ 2θ ≤ 56.88  | 3.56 ≤ 2θ ≤ 49.98   | 3.64 ≤ 2θ ≤ 50.00   | 5.90 ≤ 2θ ≤ 58.24  | 5.82 ≤ 2θ ≤ 58.44   |
| independent reflections  | 12674 [R(int) = 0.0654]  | 3663 [R(int) = 0.1039]  | 3569 [R(int) = 0.0274]  | 8420 [R(int) = 0.0281]   | 8234 [R(int) = 0.0304]  |
| data/restraints/parameters   | 12674/0/652  | 3663/0/289  | 3569/0/272  | 8420/0/451   | 8234/0/433  |
| quality-of-fit indicator <sup>c</sup>                              | 1.009  | 1.050   | 1.067   | 1.080  | 1.298   |
| final <i>R</i> indices [ <i>I</i> > 2σ( <i>I</i> )] <sup>a,b</sup> | <i>R</i> <sub>1</sub> = 0.0443, <i>wR</i> <sub>2</sub> = 0.1113                  | <i>R</i> <sub>1</sub> = 0.0598, <i>wR</i> <sub>2</sub> = 0.1469                 | <i>R</i> <sub>1</sub> = 0.0433, <i>wR</i> <sub>2</sub> = 0.1017   | <i>R</i> <sub>1</sub> = 0.0588, <i>wR</i> <sub>2</sub> = 0.1292                                | <i>R</i> <sub>1</sub> = 0.0635, <i>wR</i> <sub>2</sub> = 0.1253                 |
| <i>R</i> indices (all data)  | <i>R</i> <sub>1</sub> = 0.0919, <i>wR</i> <sub>2</sub> = 0.1252                  | <i>R</i> <sub>1</sub> = 0.0927, <i>wR</i> <sub>2</sub> = 0.1701                 | <i>R</i> <sub>1</sub> = 0.0723, <i>wR</i> <sub>2</sub> = 0.1151   | <i>R</i> <sub>1</sub> = 0.0783, <i>wR</i> <sub>2</sub> = 0.1342                                | <i>R</i> <sub>1</sub> = 0.0829, <i>wR</i> <sub>2</sub> = 0.1288                 |
| compound   | 6  | 7   | 8   | 9  | 10  |
| formula  | C <sub>20</sub> H <sub>25</sub> AgF <sub>3</sub> N <sub>5</sub> O <sub>6</sub> S | C <sub>18</sub> H <sub>21</sub> AgClN <sub>5</sub> O <sub>6</sub>               | C <sub>16</sub> H <sub>18</sub> AgClN <sub>4</sub> O <sub>6</sub> | C <sub>50</sub> H <sub>56</sub> Ag <sub>2</sub> N <sub>10</sub> O <sub>10</sub> S <sub>2</sub> | C <sub>23</sub> H <sub>25</sub> AgN <sub>4</sub> O <sub>5</sub> S               |
| fw   | 628.38   | 546.72  | 505.66  | 1236.91  | 577.40  |
| crystal system   | triclinic  | monoclinic  | monoclinic  | triclinic  | monoclinic  |
| space group  | P $\bar{1}$  | P <sub>2</sub> <sub>1</sub> /c  | C <sub>2</sub> /c   | P $\bar{1}$  | P <sub>2</sub> <sub>1</sub> /c  |
| <i>a</i> , Å   | 13.0295(5)   | 11.3404(8)  | 25.3479(18)   | 9.0376(3)  | 12.2142(15)   |
| <i>b</i> , Å   | 14.1039(6)   | 13.1353(8)  | 5.0801(5)   | 12.7047(6)   | 15.7923(18)   |
| <i>c</i> , Å   | 14.5684(6)   | 13.8734(5)  | 14.1456(16)   | 12.8359(6)   | 13.3706(17)   |
| $\alpha$ , °   | 82.237(2)  | 90  | 90  | 112.557(4)   | 90  |
| $\beta$ , °  | 88.474(2)  | 90.352(4)   | 98.728(9)   | 98.844(3)  | 112.293(8)  |
| $\gamma$ , °   | 71.598(2)  | 90  | 90  | 100.564(4)   | 90  |
| <i>V</i> , Å <sup>3</sup>  | 2516.64(18)  | 2066.5(2)   | 1800.4(3)   | 1296.60(10)  | 2386.3(5)   |
| <i>Z</i>   | 4  | 4   | 4   | 1  | 4   |
| <i>D</i> <sub>calcd</sub> , g/cm <sup>3</sup>                      | 1.658  | 1.757   | 1.865   | 1.584  | 1.607   |
| <i>F</i> (000)   | 1272   | 1104  | 1016  | 632  | 1176  |
| $\mu$ (Mo K <sub>α</sub> ), mm <sup>-1</sup>                       | 0.951  | 1.152   | 1.312   | 0.904  | 0.974   |
| range (2θ) for data collection, deg                                | 3.08 ≤ 2θ ≤ 56.68  | 5.56 ≤ 2θ ≤ 58.6  | 5.82 ≤ 2θ ≤ 50.02   | 6.02 ≤ 2θ ≤ 58.42  | 4.18 ≤ 2θ ≤ 50.00   |
| independent reflections  | 12257 [R(int) = 0.0507]  | 4752 [R(int) = 0.0287]  | 1581 [R(int) = 0.0153]  | 5942 [R(int) = 0.0254]   | 4177 [R(int) = 0.0284]  |
| data/restraints/parameters   | 12257/2/677  | 4752/0/281  | 1581/0/129  | 5942/0/319   | 4177/0/316  |
| quality-of-fit indicator <sup>c</sup>                              | 1.043  | 1.011   | 1.091   | 0.977  | 1.058   |
| final <i>R</i> indices [ <i>I</i> > 2σ( <i>I</i> )] <sup>a,b</sup> | <i>R</i> <sub>1</sub> = 0.0520, <i>wR</i> <sub>2</sub> = 0.1501                  | <i>R</i> <sub>1</sub> = 0.0343, <i>wR</i> <sub>2</sub> = 0.0565                 | <i>R</i> <sub>1</sub> = 0.0281, <i>wR</i> <sub>2</sub> = 0.0803   | <i>R</i> <sub>1</sub> = 0.0314, <i>wR</i> <sub>2</sub> = 0.0750                                | <i>R</i> <sub>1</sub> = 0.0369, <i>wR</i> <sub>2</sub> = 0.0798                 |
| <i>R</i> indices (all data)  | <i>R</i> <sub>1</sub> = 0.0820, <i>wR</i> <sub>2</sub> = 0.1682                  | <i>R</i> <sub>1</sub> = 0.0570, <i>wR</i> <sub>2</sub> = 0.0586                 | <i>R</i> <sub>1</sub> = 0.0300, <i>wR</i> <sub>2</sub> = 0.0820   | <i>R</i> <sub>1</sub> = 0.0418, <i>wR</i> <sub>2</sub> = 0.0771                                | <i>R</i> <sub>1</sub> = 0.0554, <i>wR</i> <sub>2</sub> = 0.0885                 |

<sup>a</sup>*R*<sub>1</sub> =  $\sum |F_o| - |F_c| / \sum |F_o|$ . <sup>b</sup>*wR*<sub>2</sub> =  $[\sum w(F_o^2 - F_c^2)^2 / \sum w(F_o^2)]^{1/2}$ . *w* =  $1 / [\sigma^2(F_o^2) + (ap)^2 + (bp)]$ , *p* =  $[\max(F_o^2 \text{ or } 0) + 2(F_c^2)] / 3$ . *a* = 0.0544, *b* = 0.0000, **1**; *a* = 0.1032, *b* = 1.4592, **2**; *a* = 0.0497, *b* = 1.4722, **3**; *a* = 0.0391, *b* = 15.7651, **4**; *a* = 0.0000, *b* = 17.1757, **5**; *a* = 0.0932, *b* = 0.8856, **6**; *a* = 0.0191, *b* = 0, **7**; *a* = 0.0448, *b* = 2.8372, **8**; *a* = 0.0450, *b* = 0, **9**; *a* = 0.0262, *b* = 2.617, **10**. <sup>c</sup>Quality-of-fit =  $[\sum w(|F_o^2| - |F_c^2|)^2 / (N_{\text{observed}} - N_{\text{parameters}})]^{1/2}$ .

bonds and C—H---Ag [H---Ag = 3.284(2) Å] interactions, respectively. Intermolecular Ag---O [2.763(2) Å] and C—H---O [H---O = 2.392(2) Å;  $\angle$ C—H---O = 132.5(2)°] interactions to the amide oxygen atom of the L ligands are also observed. All the Ag---O distances shown in **7–9** are outside the typical range of 2.3–2.6 Å for the Ag—O bond,<sup>10</sup> but shorter than the

corresponding van der Waals contacts which is 3.24 Å (van der Waals radius for Ag = 1.72 and O = 1.52),<sup>11</sup> indicating the formation of Ag---O interactions.

In complex **10**, the silver(I) metal centers are bridged by two pyridyl nitrogen atoms to form a metallocycle (ring size = 16.10 × 10.53 Å<sup>2</sup>), which are also coordinated by the amide oxygen

**Table 2. Selected Bond Distances (Å) and Angles (°) for 1–10<sup>a</sup>**

| 1           |            |                  |            |
|-------------|------------|------------------|------------|
| Ag(1)–N(1)  | 2.179(2)   | N(1A)–Ag(1)–N(1) | 180.0(0)   |
| Ag(1)–N(1A) | 2.179(2)   | N(5)–Ag(2)–N(4)  | 174.3(1)   |
| Ag(2)–N(4)  | 2.161(2)   | N(8B)–Ag(3)–N(8) | 180.0(0)   |
| Ag(2)–N(5)  | 2.159(2)   |                  |            |
| Ag(3)–N(8)  | 2.205(3)   |                  |            |
| Ag(3)–N(8B) | 2.205(3)   |                  |            |
| 2           |            |                  |            |
| Ag–N(1)     | 2.172(5)   | N(4A)–Ag–N(1)    | 173.0(2)   |
| Ag–N(4A)    | 2.170(5)   |                  |            |
| 3           |            |                  |            |
| Ag–N(1)     | 2.170(4)   | N(1)–Ag–N(4A)    | 175.6(2)   |
| Ag–N(4A)    | 2.174(4)   |                  |            |
| 4           |            |                  |            |
| Ag–N(1)     | 2.142(3)   | N(1)–Ag–N(4A)    | 174.8(1)   |
| Ag–N(4A)    | 2.136(3)   |                  |            |
| 5           |            |                  |            |
| Ag–N(1)     | 2.131(3)   | N(1)–Ag–N(4A)    | 176.3(1)   |
| Ag–N(4A)    | 2.136(3)   |                  |            |
| 6           |            |                  |            |
| Ag(1)–N(1)  | 2.153(3)   | N(1)–Ag(1)–N(8A) | 165.1(1)   |
| Ag(1)–N(8A) | 2.164(3)   | N(5)–Ag(2)–N(4)  | 176.5(1)   |
| Ag(2)–N(4)  | 2.147(3)   |                  |            |
| Ag(2)–N(5)  | 2.145(3)   |                  |            |
| 7           |            |                  |            |
| Ag–N(1)     | 2.155(2)   | N(4A)–Ag–N(1)    | 172.86(9)  |
| Ag–N(4A)    | 2.153(2)   |                  |            |
| 8           |            |                  |            |
| Ag–N(1)     | 2.193(2)   | N(1A)–Ag–N(1)    | 180.00(15) |
| 9           |            |                  |            |
| Ag–N(1)     | 2.1673(19) | N(4A)–Ag–N(1)    | 164.15(7)  |
| Ag–N(4A)    | 2.160(2)   |                  |            |
| 10          |            |                  |            |
| Ag–N(1)     | 2.218(3)   | N(4A)–Ag–N(1)    | 134.83(11) |
| Ag–N(4A)    | 2.201(3)   | N(1)–Ag–O(2B)    | 100.96(10) |
| Ag–O(2B)    | 2.552(3)   | N(4A)–Ag–O(2B)   | 90.99(10)  |
| Ag–O(3)     | 2.347(15)  | N(1)–Ag–O(3)     | 96.9(5)    |
|             |            | N(4A)–Ag–O(3)    | 126.1(4)   |
|             |            | O(3)–Ag–O(2B)    | 93.2(4)    |

<sup>a</sup>Symmetry transformations used to generate equivalent atoms: (A) 4 – x, 5 – y, 4 – z; (B) 1 – x, 1 – y, 2 – z for 1. (A) –1 + x, 1 + y, z; (B) –1 + x, 3 – y, –z for 2 and 3. (A) 1 + x, y, –1 + z for 4 and 5. (A) 1 + x, 1 + y, –2 + z; (B) –x, –2 + y, 4 – z for 6.

[Ag–O(2B) = 2.552 (3) Å] atoms to form a 2D pleated grid with a {4,8<sup>2</sup>} topology, Figure 3c. Each silver(I) metal center is also coordinated by one *p*-TsO<sup>−</sup> anion [Ag–O(3) = 2.347(15) Å] through the oxygen atom, resulting in a distorted trigonal pyramidal coordination geometry, with the silver(I) center deviating from the plane by 0.31 Å. Noticeably, the Ag–O distances of 2.552 (3) and 2.347(15) Å fall in the range of 2.3–2.6 Å for a Ag–O bond. Figure 4 depicts a drawing showing the structural transformation from 9 to 10 upon removal of the acetonitrile molecules.

**Conformations of the Ligands.** It has been shown that *N,N'*-di(2-pyridyl)adipoamide can be arranged in *anti-anti-anti* (AAA), *anti-anti-gauche* (AAG), *anti-gauche-anti* (AGA), *anti-gauche-gauche* (AGG), *gauche-anti-gauche* (GAG), and *gauche-gauche-gauche* (GGG) conformations, and based on the relative orientation of the C=O (or N–H) groups, each conformation can adopt a *cis* or *trans* arrangement.<sup>7a</sup> The A and G

conformations are given when the C–C–C–C torsion angle ( $\theta$ ) is  $180 \geq \theta > 90^\circ$  and  $0 \leq \theta \leq 90^\circ$ , respectively. According to this descriptor, the L ligands of complexes 1–7 can be assigned as AAA *trans* and those in complexes 8–10 as AAA *trans*, AGG *cis*, and AGA *cis*, respectively. Noticeably, due to the difference in the orientations of the pyridyl nitrogen atom positions, three more orientations, *anti-anti*, *syn-anti*, and *syn-syn*, based on the relative positions of the pyridyl nitrogen and amide oxygen atom, are possible for the L ligand, Figure 5. Table 3 lists the ligand conformation found for complexes 1–10. The L ligands in the 1D concavo-convex chain complex 1 adopt the AAA *trans syn-anti* conformation, while those in the 1D zigzag chain complexes 2–7 adopt the AAA *trans syn-syn* conformation and those in complexes 8–10 adopt the AAA *trans anti-anti*, AGG *cis anti-anti*, and AGA *cis anti-anti* conformations, respectively. These ligand conformations also differ in the dihedral angle ( $0$ – $88.2^\circ$ ) between the two pyridyl rings; that is, the two pyridyl rings are coplanar or twisted about the C–N bonds. A structural comparison between 7 and 8 shows that removal of acetonitrile molecules from 7 results in a significant change in the ligand conformation. The similar situation applies to 9 and 10.

### Structural Comparisons and Ag–Ag Distances.

Structural comparisons of 1–10 show that the interplay of solvents and counteranions is important in determining the structural diversity. For complexes with the CH<sub>3</sub>CN solvents, 1–3 and 7, the octahedral PF<sub>6</sub><sup>−</sup> anions induce the 1D concavo-convex chains, while the tetrahedral BF<sub>4</sub><sup>−</sup> and ClO<sub>4</sub><sup>−</sup> anions and triangular NO<sub>3</sub><sup>−</sup> anions direct the 1D zigzag chains. For complexes with the DMF solvents, 4–6, all the complexes adopt the 1D zigzag chains. The 1D zigzag chains in 2, 3, 6, and 7 are also supported by the Ag–Ag and  $\pi$ – $\pi$  interactions to form 1D polymeric pairs. Noticeably, the *p*-TsO<sup>−</sup> anions in 9 and 10 play different structural roles as compared with the anions in the other complexes, resulting in a 0D metallocycle and 2D pleated grid, respectively. Complexes 2, 3, and 7 make interesting comparisons with the Ag(I) complexes containing *N,N'*-di(2-pyridyl)adipoamide (L'), involving [Ag(L')(NO<sub>3</sub>)]<sub>∞</sub>, [Ag(L')(BF<sub>4</sub>)(CH<sub>3</sub>CN)(H<sub>2</sub>O)<sub>0.5</sub>]<sub>∞</sub>, and [Ag(L')(ClO<sub>4</sub>)(CH<sub>3</sub>CN)]<sub>∞</sub>.<sup>7a</sup> All six complexes form 1D zigzag chains. While the zigzag chains of the three complexes containing the L' ligands are interlinked through Ag–O and N–H–N interactions, those of 2, 3, and 7 are supported by the Ag–Ag and  $\pi$ – $\pi$  interactions to form 1D polymeric pairs. This result indicates that the ligand-isomerism of the spacer ligand plays a more important role than the NO<sub>3</sub><sup>−</sup>, BF<sub>4</sub><sup>−</sup>, and ClO<sub>4</sub><sup>−</sup> anions in determining the supramolecular structures. Noticeably, all L and L' in these six complexes adopt the AAA *trans* conformation to form the 1D zigzag chains.

The closed-shell Ag–Ag interaction (argentophilicity)<sup>12</sup> can be either ligand-supported<sup>13</sup> or ligand-unsupported<sup>14</sup> by the ancillary ligands and its strength is comparable to a weak hydrogen bond.<sup>15</sup> Most short Ag–Ag distances were observed in the structurally characterized complexes with bridging ligands (ligand supported), and the attractive phenomenon was generally accepted after examples of ligand-unsupported Ag–Ag interactions were reported.<sup>16</sup> Table 4 lists the Ag–Ag and  $\pi$ – $\pi$  distances found in complexes 2, 3, 6, and 7 which show 1D polymeric pairs supported by the Ag–Ag and  $\pi$ – $\pi$  interactions. The Ag–Ag distances of these complexes are significantly shorter than the sum of the van der Waals radius (3.44 Å) of Ag atom,<sup>11</sup> indicating the formation of Ag–Ag interaction. The  $\pi$ – $\pi$  distances are also shorter than the typical

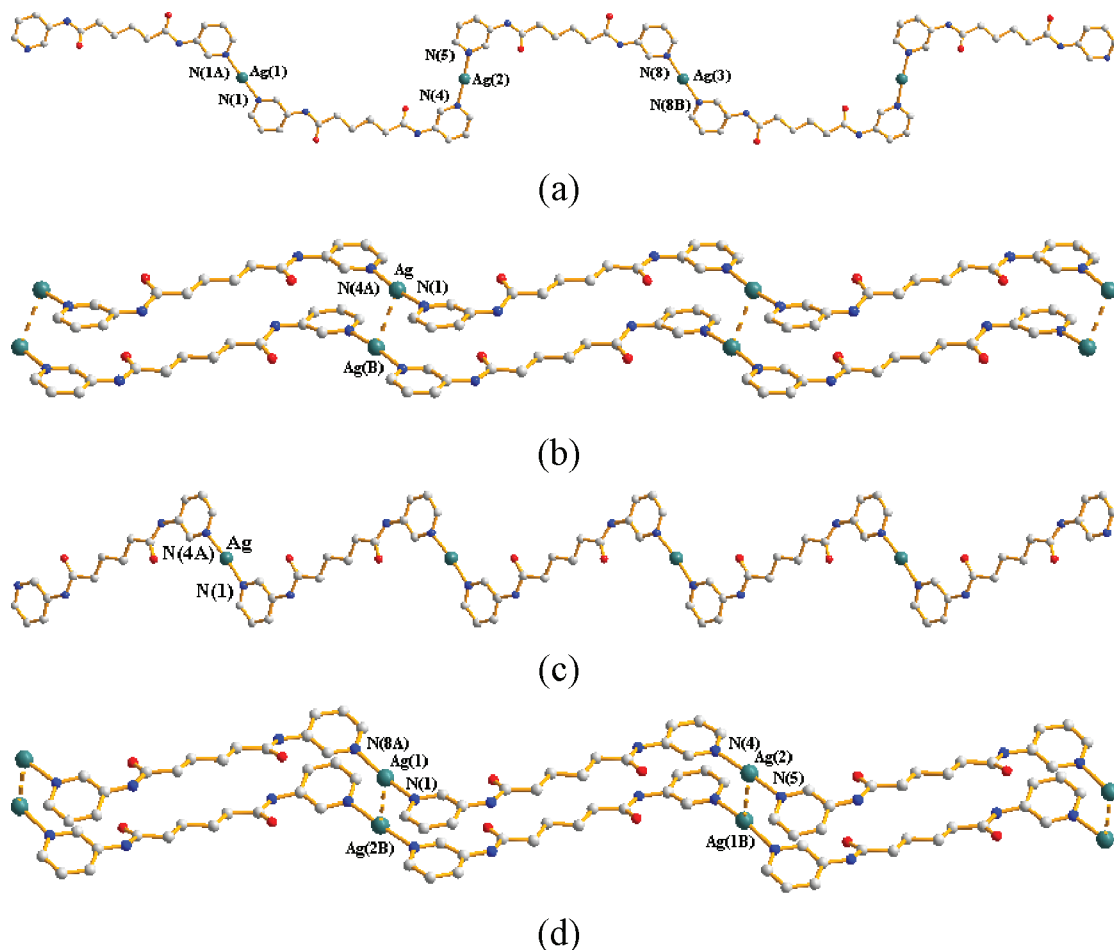


**Figure 1.** (a) The 1D concavo-convex cationic chain of complex 1. Symmetry transformations used to generate equivalent atoms: (A)  $4 - x, 5 - y, 4 - z$ ; (B)  $1 - x, 1 - y, 2 - z$  for 1. (b) A representative drawing showing the 1D polymeric pair of 2 and 3. Symmetry transformations used to generate equivalent atoms: (A)  $-1 + x, 1 + y, z$ ; (B)  $-1 + x, 3 - y, -z$ . (c) A representative drawing showing the zigzag chain of 4 and 5. Symmetry transformations used to generate equivalent atoms: (A)  $1 + x, y, -1 + z$ . (d) The 1D polymeric pair of complex 6. Symmetry transformations used to generate equivalent atoms: (A)  $1 + x, 1 + y, -2 + z$ ; (B)  $-x, -2 + y, 4 - z$  for 6.

cutoff distance for  $\pi-\pi$  stacking interactions which is  $3.9 \text{ \AA}^{17}$ . These short Ag---Ag contacts can be regarded as ligand-unsupported; however, they are supported by the head-to-head  $\pi-\pi$  stacking interactions between the pyridyl rings. Noticeably, the shorter Ag---Ag distances in complexes 6 and 7 are supported by the shorter  $\pi-\pi$  contacts, although weak interactions such as C---H---F and N---H---O hydrogen bonds and Ag---O and Ag---N interactions may play important roles in determining these ligand-unsupported Ag---Ag distances.

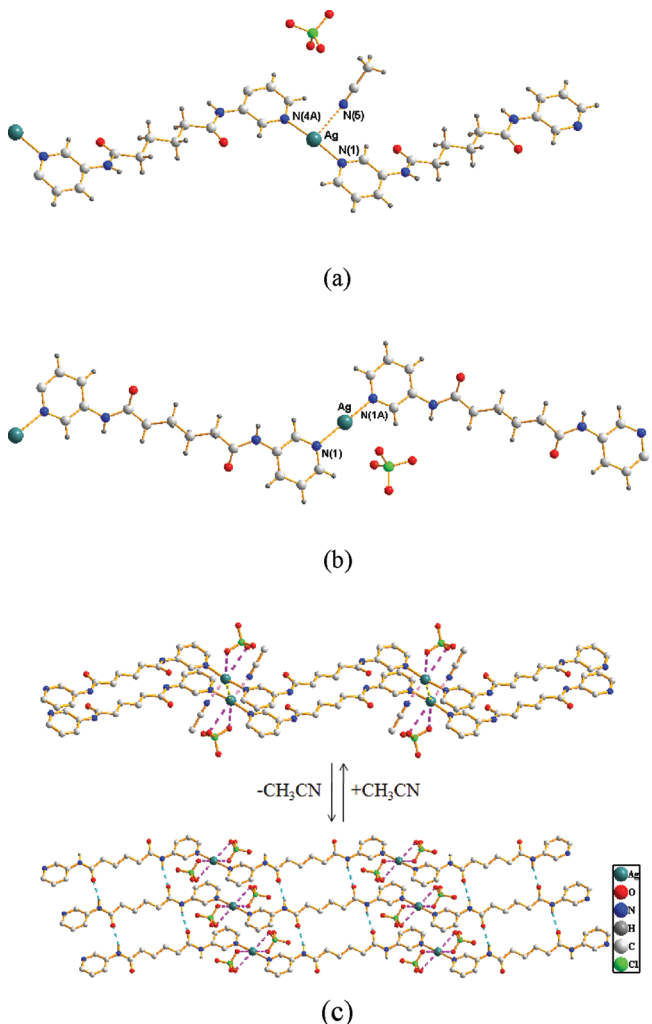
**Thermal Properties.** Thermal gravimetric analyses (TGA) were carried out to examine the thermal stabilities of 1–10. Figure S7, Supporting Information shows the TGA curves for 1–6. A comparison of the curves shows that for complexes with the same counteranions (1 and 4; 2 and 5), the DMF molecules in 5 are more thermally stable than the  $\text{CH}_3\text{CN}$  molecules in 2, but the difference between 1 and 4 is not significant. This result indicates that the  $\text{PF}_6^-$  anions govern the supramolecular interactions in 1 and 4, whereas the DMF molecules in 5 play the more important role.

Figure 6 shows the TGA curves for 7–10. The most striking feature of this figure is that the TGA curves of 7 and 8 can be superimposed at the temperatures above  $200^\circ\text{C}$ , indicating the possible transformation from 7 to 8 upon removal of the

acetonitrile molecules. Similar superimposition at the temperatures above  $140^\circ\text{C}$  is also observed for 9 and 10.

**Crystal-to-Crystal Transformation.** Crystal-to-crystal transformation of metal complexes is an interesting phenomenon for their potential applications as switches and sensors.<sup>18</sup> However, crystal-to-crystal transformations involving coordination polymers are rare since they involve breaking and forming of coordinate and/or covalent bonds in more than one direction.<sup>18a</sup> Despite some recent progress, the ability to predict and control the transformation remains an elusive goal, and much more work is required for elucidating the details of such interesting phenomena.

Complexes 7–10 provide an unique opportunity to investigate the structural transformations due to solvent removal in the silver(I) complexes containing the flexible dipyridyl amide ligands. To confirm the transformations in 7–10, we first checked their purities by measuring the PXRD patterns. Figures S8 and S9 show that the powder patterns of these four complexes match quite well with those simulated from single-crystal X-ray data, indicating the bulk purities of these complexes. We then measured the variable temperature PXRD patterns of 7, Figure 7, showing that the patterns of 7 start to change from  $130^\circ\text{C}$  and become similar to that for complex 8 at  $180^\circ\text{C}$ . At  $200^\circ\text{C}$ , the sample is desolvated and the powder pattern matches quite well with that of



**Figure 2.** (a) Coordination environment of the silver(I) center in **7**. Symmetry transformations used to generate equivalent atoms: (A)  $x - 1, y - 1, z$ . (b) Coordination environment of the silver(I) center in **8**. Symmetry transformations used to generate equivalent atoms: (A)  $-x + 1, -y, -z$ . (c) A drawing showing the transformation between **7** and **8**.

complex **8**, indicating the crystal-to-crystal transformation from **7** to **8**. Noticeably, when the desolvated sample was exposed to  $\text{CH}_3\text{CN}$  vapor, that is, the dry sample was placed in a glass desiccator beside a beaker filled with  $\text{CH}_3\text{CN}$ , it reabsorbed the lost  $\text{CH}_3\text{CN}$ . The PXRD pattern of the resolvated species, Figure S8e, is almost the same as that of the freshly synthesized material, suggesting that the original crystalline phase of **7** was regenerated. The transformation from **7** to **8** is thus reversible. As shown in Figure 2a–c, the reversible structural transformations between **7** and **8** upon removal and uptake of the acetonitrile molecules result in significant changes in the geometries of the silver(I) metal centers, ligand conformations, and supramolecular structures. We have also investigated the possibility of absorption or coordination of other common organic solvents (dichloromethane, tetrahydrofuran, ethanol, toluene, DMF) for compound **8**, but none of these solvent molecules can be accommodated into its structure, showing the specific selectivity of **8**.

The variable temperature powder X-ray diffraction patterns of **9**, Figure 8, shows that a significant change of the pattern is observed at  $140^\circ\text{C}$ . At  $200^\circ\text{C}$ , the sample is desolvated and the powder pattern matches quite well with that of complex **10**.

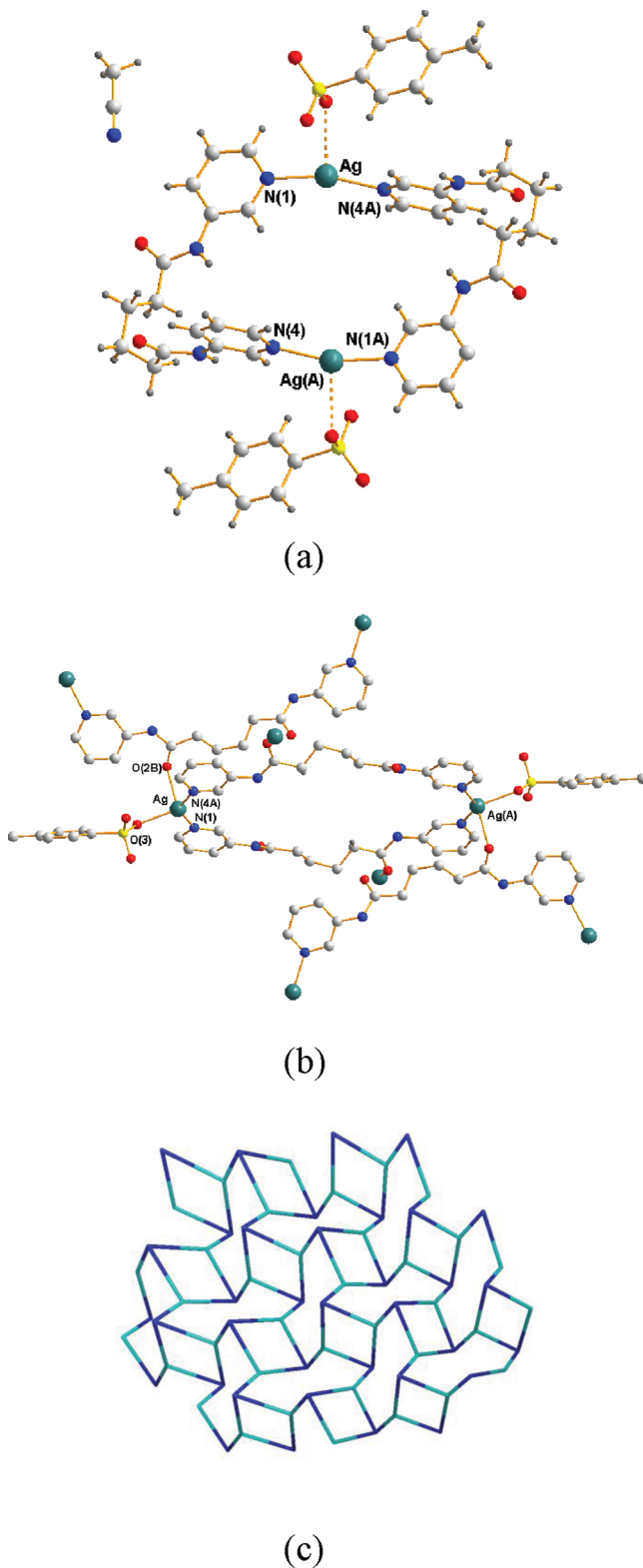


**Figure 3.** (a) Coordination environment of the silver(I) center in **9**. Symmetry transformations used to generate equivalent atoms: (A)  $-x + 2, -y + 2, -z + 1$ . (b) Coordination environment of the silver(I) center in **10**. Symmetry transformations used to generate equivalent atoms: (A)  $-x + 1, -y, -z + 3$ ; (B)  $-x + 1, y + 1/2, -z + 5/2$  for **10**. (c) A figure showing the  $\{4,8^2\}$  topology of **10**.

However, attempts to resolvate **9** to obtain **10** have not been successful. The desolvation process from **9** to **10** is therefore irreversible. The irreversible transformation between **9** and **10**

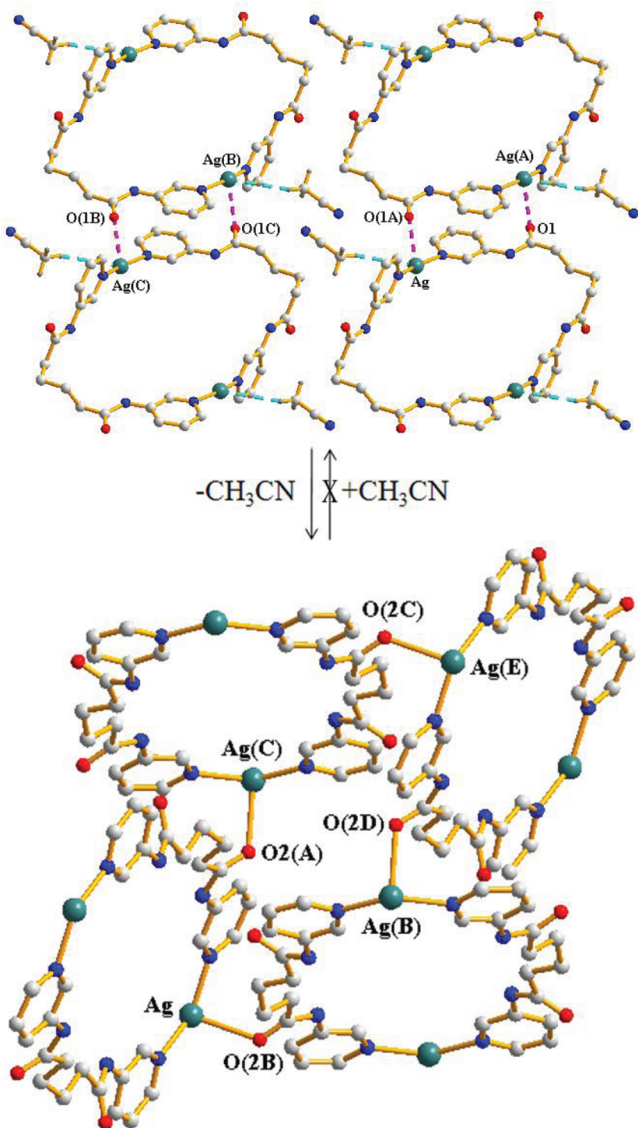


**Figure 4.** A drawing showing the transformation between **9**, top, and **10**, bottom. The  $p\text{-TsO}^-$  anions are removed for clarity. Symmetry transformations used to generate equivalent atoms: (A)  $-x + 2, -y + 2, -z + 1$ ; (B)  $-x + 1, -y + 2, -z + 2$ ; (C)  $x - 1, y, z + 1$  for **9**; (A)  $-x + 1, -y, -z + 3$ ; (B)  $-x + 1, y + 1/2, -z + 5/2$ ; (C)  $x, -y + 1/2, z + 1/2$ ; (D)  $x, y + 1, z$ ; (E)  $-x + 1, -y + 1, -z + 3$  for **10**.

can be ascribed to the formation of the Ag–O coordinate bonds to the amide oxygen atoms of the L ligands and those to the sulfonate oxygen atoms of the  $p\text{-TsO}$  anions in **10**, which are not breakable upon attack of the acetonitrile molecules to the silver(I) metal centers, Figure 4.

**Luminescent Properties.** Luminescent metal complexes are interesting owing to their ability to enhance, shift, and quench luminescent emission of organic ligands by metal coordination. Usually, the emission bands of silver(I) coordination polymers may originate from  $n \rightarrow \pi^*$ ,  $\pi \rightarrow \pi^*$  intraligand or ligand-to-metal charge transfer (LMCT) transitions.<sup>19</sup> Figure 9a,b shows the emission spectra of the free ligand L and complexes **1–10**, which were measured in the solid at room temperature, and Table 5 list the corresponding excitation and emission wavelengths. In the solid state, the free L ligand exhibits photoluminescence with an emission maximum at 415 nm upon excitation at 376 nm. Since the emission

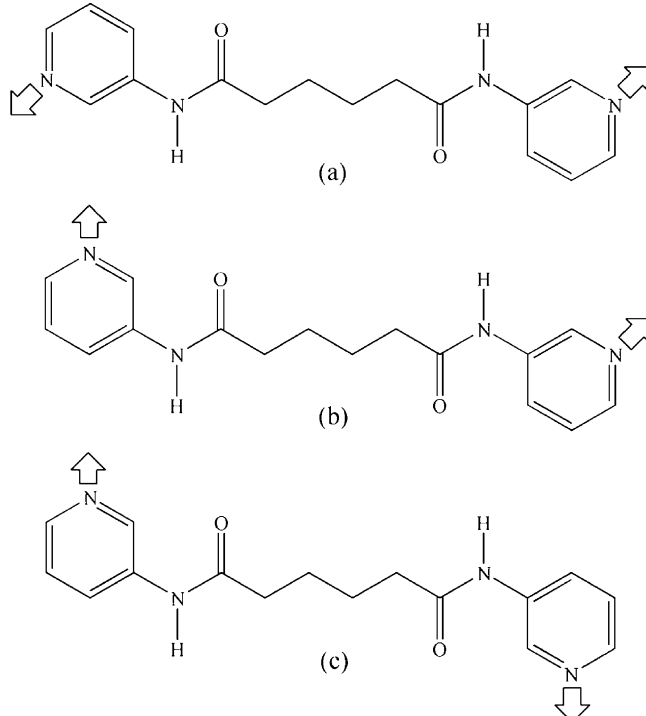


**Figure 5.** Three possible orientations for the pyridyl nitrogen atoms of the L ligand. (a) *anti-anti*, (b) *syn-anti*, (c) *syn-syn*.

**Table 3.** Ligand Conformations and Corresponding Angles for Complexes **1–10**

| compound  | torsion angle ( $^\circ$ ) | conformation               | dihedral angle ( $^\circ$ ) |
|-----------|----------------------------|----------------------------|-----------------------------|
| <b>1</b>  | 172.3, 175.9, 177.1        | AAA <i>trans syn-anti</i>  | 11.6                        |
|           | -173.6, 179.0, -175.2      | AAA <i>trans syn-anti</i>  | 14.8                        |
| <b>2</b>  | 179.2, -176.6, -175.4      | AAA <i>trans syn-syn</i>   | 6.5                         |
| <b>3</b>  | 174.7, 177.2, 177.7        | AAA <i>trans syn-syn</i>   | 4.2                         |
| <b>4</b>  | 176.6, -179.9, 173.7       | AAA <i>trans syn-syn</i>   | 12.3                        |
| <b>5</b>  | 173.0, 179.8, -180.0       | AAA <i>trans syn-syn</i>   | 20.3                        |
| <b>6</b>  | -173.4, -178.3, -178.9     | AAA <i>trans syn-syn</i>   | 7.6                         |
|           | -174.8, 179.3, -178.5      | AAA <i>trans syn-syn</i>   | 9.5                         |
| <b>7</b>  | -179.3, 175.2, -175.2      | AAA <i>trans syn-syn</i>   | 7.4                         |
| <b>8</b>  | 176.8, 180.0, -176.8       | AAA <i>trans anti-anti</i> | 0                           |
| <b>9</b>  | -179.0, 67.2, 69.4         | AGG <i>cis anti-anti</i>   | 88.2                        |
| <b>10</b> | -172.6, -66.5, -163.2      | AGA <i>cis anti-anti</i>   | 8.0                         |

**Table 4.** The Ag–Ag and  $\pi$ – $\pi$  Distances ( $\text{\AA}$ ) in Complexes **2**, **3**, **6**, and **7**

| complex  | Ag–Ag    | $\pi$ – $\pi$      |
|----------|----------|--------------------|
| <b>2</b> | 3.218(2) | 3.608(1)           |
| <b>3</b> | 3.391(1) | 3.593(1)           |
| <b>6</b> | 3.119(1) | 3.506(1), 3.551(1) |
| <b>7</b> | 3.140(3) | 3.544(2)           |

bands in the range 400–409 nm for **2**, **3**, **6**, **7–10** are close to the emission of the free L ligand, they may be tentatively ascribed to the intraligand (IL)  $\pi \rightarrow \pi^*$  transitions. The substantial amount of red-shift for the energy bands in 470–493 nm for **1**, **4**, **5**, and **8** is most probably due to the formation of the silver(I) polymeric complexes and may originate from the charge transition between the ligand and metal ions. There is a correlation between structures and luminescence for the 1D

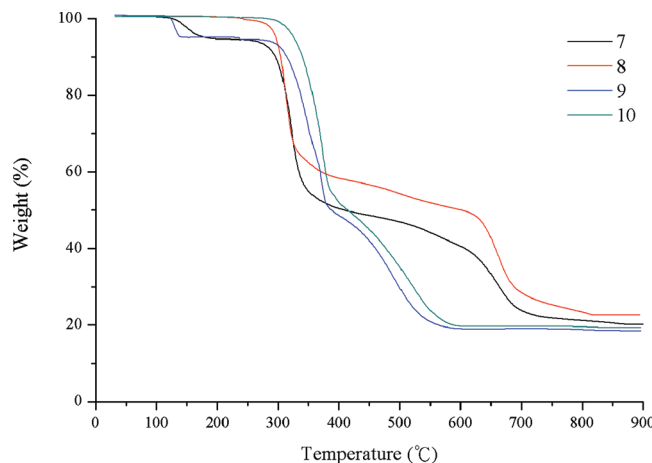


Figure 6. TGA curves for complexes 7–10.

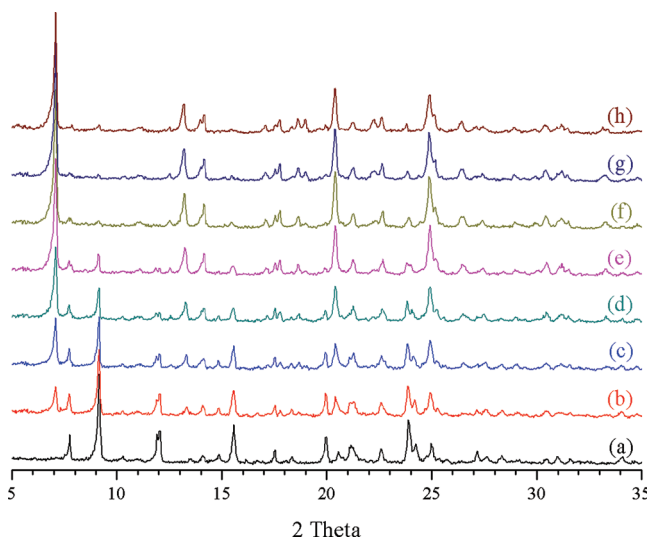


Figure 7. The XRPD patterns of complex 7 at (a) 130 °C, (b) 140 °C, (c) 150 °C, (d) 160 °C, (e) 170 °C, (f) 180 °C, (g) 190 °C, (h) 200 °C.

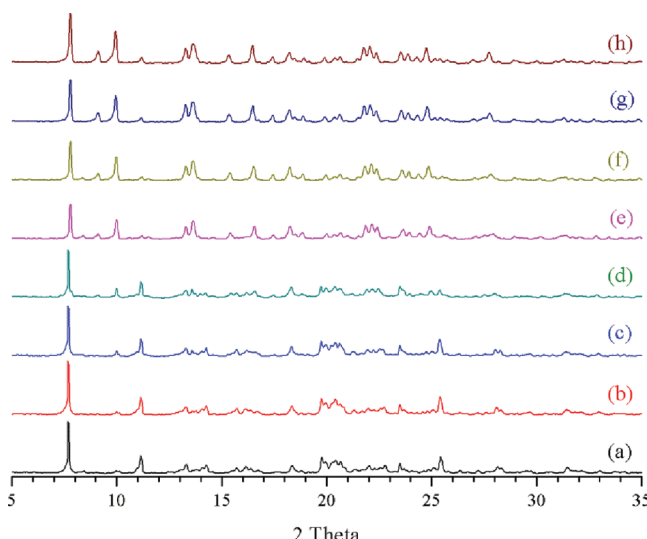


Figure 8. The XRPD patterns of complex 9 at (a) 60 °C, (b) 80 °C, (c) 100 °C, (d) 120 °C, (e) 140 °C, (f) 160 °C, (g) 180 °C, (h) 200 °C.

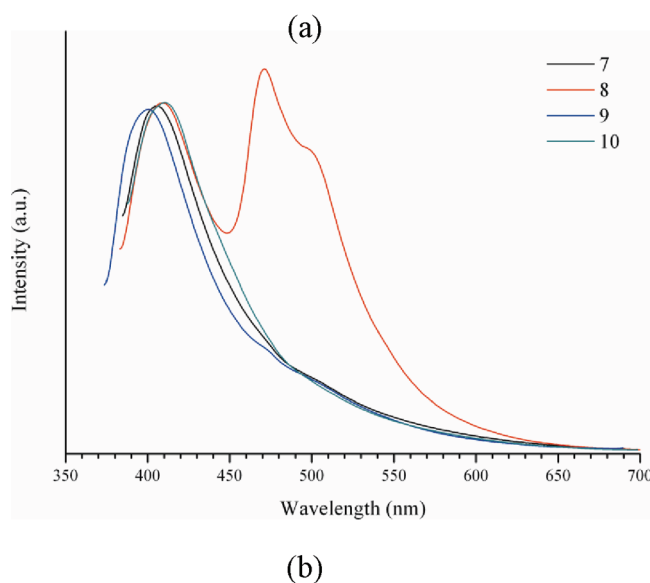
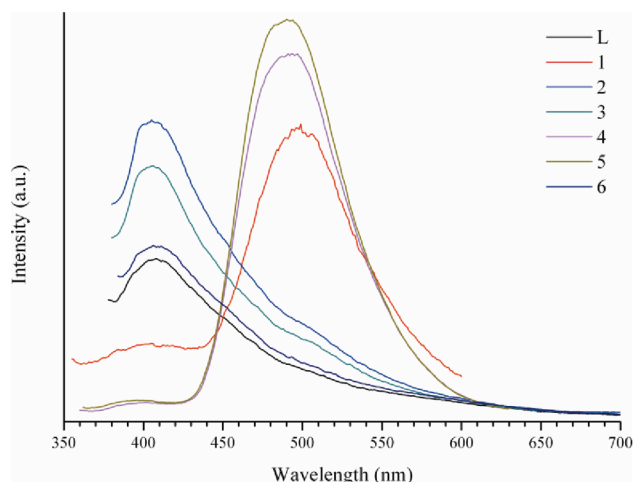


Figure 9. (a) Emission spectra of L and complexes 1–6. (b) Emission spectra of L and complexes 7–10.

Table 5. Luminescent Properties of L and 1–10 in the Solid State

| compound | $\lambda_{\text{ex}}/\lambda_{\text{em}}$ (nm) | compound | $\lambda_{\text{ex}}/\lambda_{\text{em}}$ (nm) |
|----------|--|----------|--|
| L        | 376/415  | 6        | 375/408  |
| 1        | 310/498  | 7        | 362/405  |
| 2        | 366/404  | 8        | 371/409, 470                                   |
| 3        | 365/405  | 9        | 357/400  |
| 4        | 330/493  | 10       | 370/409  |
| 5        | 320/489  |          |  |

chain complexes 1–8: Complexes 2, 3, 6, and 7 which are supported by the Ag–Ag and  $\pi$ – $\pi$  interactions show emission bands around 400 nm and those with the weak C–H–F or C–H–O intermolecular hydrogen bonds, 1, 4, and 5, show emission bands around 500 nm, whereas complex 8 which displays strong N–H–O hydrogen bonds exhibits both emissions bands. The emission wavelengths thus probably reveal the types of supramolecular interactions of the Ag(I) complexes containing the L ligands. A comparison of the emission spectra of 7 and 8 shows that the reversible transformation between them resulted in the drastic change in the luminescent properties.

## CONCLUSION

In this study, the coordination chemistry of the flexible ligand *N,N'*-di(3-pyridyl)adipoamide (**L**) with the silver(I) salts has been successfully accomplished. The anions and solvents are important in determining the structural diversity. For complexes with the CH<sub>3</sub>CN solvents, the octahedral PF<sub>6</sub><sup>-</sup> anions induce 1D concavo-convex chains, and the tetrahedral BF<sub>4</sub><sup>-</sup> and ClO<sub>4</sub><sup>-</sup> anions and the triangular NO<sub>3</sub><sup>-</sup> anions direct 1D zigzag chains, whereas the *p*-TsO<sup>-</sup> anion affords a 0D dinuclear metallocycle. For complexes with the DMF solvents, all the complexes containing the BF<sub>4</sub><sup>-</sup>, ClO<sub>4</sub><sup>-</sup>, and NO<sub>3</sub><sup>-</sup> anions adopt the 1D zigzag chains. The **L** ligands in complex **1** adopt the AAA *trans syn-anti* conformation and those in **2–7** adopt the AAA *trans syn-syn* conformation, while those in **8–10** adopt the AAA *trans anti-anti*, AGG *cis anti-anti*, and AGA *cis anti-anti* conformations, respectively, resulting in 0D metallocycle, 1D coordination polymers involving concavo-convex chains, polymeric pairs of zigzag chains supported by the Ag--Ag and  $\pi$ -- $\pi$  interactions and zigzag chains, and a 2D pleated grid. The flexibility of the **L** ligand as well as the nature of the counteranion and solvent are thus essential in determining the structural type and the **L** ligand adopts the conformation that maximizes the intra- and intermolecular forces.

Crystal-to-crystal transformation between the 1D polymeric pair **7** and the zigzag chain **8** is reversible, while the process between the 0D metallocycle **9** and the 2D pleated grid **10** is irreversible. Removal of the acetonitrile molecules facilitated the structural transformations, and the conformational change is more feasible than the breakage of the Ag–O bond. Both transformations are accompanied by the changes in the ligand conformations and supramolecular structures. Significant changes in the luminescent properties are also found for complexes **7** and **8**, which may show potential applications as sensing elements. This study also shows that the proper choice of the anions may lead to the observation of interesting crystal-to-crystal transformation.

## ASSOCIATED CONTENT

### Supporting Information

The ORTEP diagrams showing the asymmetric units of **1–6** (Figures S1–S6). TGA curves for complexes **1–6** (Figure S7). The XRPD patterns of **7–8** (Figure S8) and **9–10** (Figure S9). This material is available free of charge via the Internet at <http://pubs.acs.org>. In addition, crystallographic data (CIF files, excluding structure factors) for complexes **1–10** have been deposited with the Cambridge Crystallographic Data Centre, CCDC Nos. 850457–850462 and 826251–826254.

## AUTHOR INFORMATION

### Corresponding Author

\*E-mail: jdchen@cycu.edu.tw.

## ACKNOWLEDGMENTS

We are grateful to the National Science Council of the Republic of China for support. We also thank Miss C.-W. Lu of the Instrumentation Center, National Taiwan University, for CHNS (EA) analysis experiments.

## REFERENCES

- (a) Tiekink, E. R. T.; Vittal, J. J. *Frontiers in Crystal Engineering*; John Wiley & Sons, Ltd: England, 2006. (b) Robson, R.; Abrahams, B. E.; Batten, S. R.; Gable, R. W.; Hoskins, B. F.; Lieu, J. *Supramolecular Architecture*; ACS Publications: Washington, DC, 1992. (c) Yaghi, O. M.; Li, H.; Davis, C.; Richardson, D.; Groy, T. L. *Acc. Chem. Res.* **1998**, *31*, 474. (d) Fujita, M.; Ogura, K. *Coord. Chem. Rev.* **1996**, *148*, 249. (e) Leong, W. L.; Vittal, J. J. *Chem. Rev.* **2011**, *111*, 688.
- (2) (a) Sijbesma, R. P.; Meijer, E. W. *Curr. Opin. Colloid Interface Sci.* **1999**, *4*, 24. (b) Zimmerman, S. C.; Corbin, P. S. *Struct. Bonding (Berlin)* **2000**, *96*, 63. (c) Sherrington, D. C.; Taskinen, K. A. *Chem. Soc. Rev.* **2001**, *30*, 83. (d) Lawrence, D. S.; Jiang, T.; Levett, M. *Chem. Rev.* **1995**, *95*, 2229.
- (3) (a) Li, H.-H.; Chen, Z.-R.; Li, J.-Q.; Huang, C.-C.; Zhang, Y. F.; Jia, G.-X. *Cryst. Growth Des.* **2006**, *6*, 1813. (b) Awaleh, M. O.; Badia, A.; Brisse, F. *Cryst. Growth Des.* **2006**, *6*, 2674. (c) Noro, S.; Kitaura, R.; Kondo, M.; Kitagawa, S.; Ishii, T.; Matsuzaka, H.; Yamashita, M. *J. Am. Chem. Soc.* **2002**, *124*, 2568. (d) Wang, Y.-H.; Chu, K.-L.; Chen, H.-C.; Yeh, C.-W.; Chan, Z.-K.; Suen, M.-C.; Chen, J.-D. *CrystEngComm* **2006**, *8*, 84. (e) Lin, C.-Y.; Chan, Z.-K.; Yeh, C.-W.; Wu, C.-J.; Chen, J.-D.; Wang, J.-C. *CrystEngComm* **2006**, *8*, 841.
- (4) Bu, X. H.; Chen, W.; Hou, W. F.; Zhang, R. H.; Brisse, F. *Inorg. Chem.* **2002**, *41*, 3477.
- (5) Blake, A. J.; Champness, N. R.; Cooke, P. A.; Nicolson, J. E. B.; Wilson, C. J. *J. Chem. Soc., Dalton Trans.* **2000**, 3811.
- (6) See, for example: (a) Carlucci, L.; Ciani, G.; Proserpio, D. M.; Rizzato, S. *CrystEngComm* **2002**, *4*, 121. (b) Awaleh, M. O.; Badia, A.; Brisse, F. *Inorg. Chem.* **2005**, *44*, 7833. (c) Awaleh, M. O.; Badia, A.; Brisse, F. *Cryst. Growth Des.* **2005**, *5*, 1897. (d) Du, M.; Li, C.-P.; Zhao, X.-J. *Cryst. Growth Des.* **2006**, *6*, 335. (e) Xia, Y.; Li, S.; Wu, B.; Liu, Y.; Yang, X.-J. *CrystEngComm* **2001**, *13*, 5763. (f) Pigge, F. C. *CrystEngComm* **2011**, *13*, 1733.
- (7) (a) Chen, H.-C.; Hu, H.-L.; Chan, Z.-K.; Yeh, C.-W.; Jia, H.-W.; Wu, C.-P.; Chen, J.-D.; Wang, J.-C. *Cryst. Growth Des.* **2007**, *7*, 698. (b) Hsu, Y.-F.; Lin, C.-H.; Chen, J.-D.; Wang, J.-C. *Cryst. Growth Des.* **2008**, *8*, 1094. (c) Hsu, Y.-F.; Hu, H.-L.; Wu, C.-J.; Yeh, C.-W.; Proserpio, D. M.; Chen, J.-D. *CrystEngComm* **2009**, *11*, 168. (d) Hsu, Y.-F.; Hsu, W.; Wu, C.-J.; Cheng, P.-C.; Yeh, C.-W.; Chang, W.-J.; Chen, J.-D.; Wang, J.-C. *CrystEngComm* **2010**, *12*, 702.
- (8) (a) XSCANS, Release, 2.1; Siemens Energy & Automation, Inc.; Madison, Wisconsin, USA, 1995. (b) SMART/SAINT/ASTRO, Release 4.03; Siemens Energy & Automation, Inc.: Madison, Wisconsin, USA, 1995.
- (9) Sheldrick, G. M. *Acta Crystallogr.* **2008**, *A64*, 112.
- (10) Muthu, S.; Yip, J. H. K.; Vittal, J. J. *J. Chem. Soc., Dalton Trans.* **2002**, 4561.
- (11) Bondi, A. *J. Phys. Chem.* **1964**, *68*, 441.
- (12) Pyykkö, P. *Chem. Rev.* **1997**, *97*, 597.
- (13) (a) Guo, G.-C.; Zhou, G.-D.; Wang, Q.-G.; Mak, T. C. W. *Angew. Chem., Int. Ed.* **1998**, *37*, 630. (b) Che, C.-M.; Tse, M.-C.; Chan, M. C. W.; Cheung, K.-K.; Phillips, D. L.; Leung, K.-H. *J. Am. Chem. Soc.* **2000**, *122*, 2464. (c) Nomiya, K.; Takahashi, S.; Noguchi, R.; Netmoto, S.; Takayama, T.; Oda, M. *Inorg. Chem.* **2000**, *39*, 3301. (d) Djordjević, B.; Schuster, O.; Schmidbaur, H. *Inorg. Chem.* **2005**, *44*, 673. (e) Reger, D. L.; Semeniuc, R. F.; Captain, B.; Smith, M. D. *Inorg. Chem.* **2005**, *44*, 2995. (f) Zang, S.-Q.; Zhao, L.; Mak, T. C. W. *Organometallics* **2008**, *27*, 2396. (g) Rim, C.; Zhang, H.; Son, D. Y. *Inorg. Chem.* **2008**, *47*, 11993.
- (14) (a) Yaghi, O. M.; Li, H. *J. Am. Chem. Soc.* **1996**, *118*, 295. (b) Singh, K.; Long, J. R.; Stavropoulos, P. *J. Am. Chem. Soc.* **1997**, *119*, 2942. (c) Omary, M. A.; Webb, T. R.; Assefa, Z.; Shankle, G. E.; Patterson, H. H. *Inorg. Chem.* **1998**, *37*, 1380. (d) Jung, O.-S.; Lee, Y.-A.; Kim, Y. J.; Hong, J. *Cryst. Growth Des.* **2002**, *2*, 497. (e) Liu, X.; Guo, G.-C.; Fu, M.-L.; Liu, X.-H.; Wang, M.-S.; Huang, J.-S. *Inorg. Chem.* **2006**, *45*, 3679. (f) Madalan, A. M.; Avarvari, N.; Andruh, M. *Cryst. Growth Des.* **2006**, *6*, 1671. (g) Ray, L.; Shaikh, M. M.; Ghosh, P. *Inorg. Chem.* **2008**, *47*, 230.
- (15) (a) Harwell, D. E.; Mortimer, M. D.; Knobler, C. B.; Anet, F. A. L.; Hawthorne, M. F. *J. Am. Chem. Soc.* **1996**, *118*, 2679. (b) Braga, D.; Gerpioni, F.; Desiraju, G. *Chem. Rev.* **1998**, *98*, 1375. (c) Hunks, W. J.; Jennings, M. C.; Puddephatt, R. J. *Inorg. Chem.* **2000**, *39*, 2699. (d) Smyth, D. R.; Hester, J.; Young, V. G. Jr.; Tiekink, E. R. T. *CrystEngComm* **2002**, *4*, 517.

- (16) Singh, K. S.; Long, J. R.; Stavropoulos, P. *J. Am. Chem. Soc.* **1997**, *119*, 2942.
- (17) Nattinen, K. I.; Rissanen, K. *Cryst. Growth Des.* **2003**, *3*, 339.
- (18) (a) Vittal, J. J. *Coord. Chem. Rev.* **2007**, *251*, 1781. (b) Chen, C. L.; Beatty, A. M. *J. Am. Chem. Soc.* **2008**, *130*, 17222. (c) Sadeghzadeh, H.; Morsali, A. *Inorg. Chem.* **2009**, *48*, 10871. (d) Duan, Z.; Zhang, Y.; Zhang, B.; Zhu, D. *J. Am. Chem. Soc.* **2009**, *131*, 6934. (e) Aslani, A.; Morsali, A.; Zeller, M. *Dalton Trans.* **2008**, 5173. (f) Mahmoudi, G.; Morsali, A. Z. *Anorg. Allg. Chem.* **2009**, *635*, 2697. (g) Uemura, K.; Saito, K.; Kitagawa, S.; Kita, H. *J. Am. Chem. Soc.* **2006**, *128*, 16122. (h) Nather, C.; Bhosekar, G.; Jess, I. *Inorg. Chem.* **2007**, *46*, 8079. (i) Zhang, B.; Zhu, D.; Zhang, Y. *Chem.—Eur. J.* **2010**, *16*, 9994. (j) Zhang, Y.-J.; Liu, T.; Kanegawa, S.; Sato, O. *J. Am. Chem. Soc.* **2010**, *132*, 912. (k) Zhang, Y.-J.; Liu, T.; Kanegawa, S.; Sato, O. *J. Am. Chem. Soc.* **2009**, *131*, 7942. (l) Cheng, X.-N.; Zhang, W.-X.; Chen, X.-M. *J. Am. Chem. Soc.* **2007**, *129*, 15738.
- (19) Chen, C.-L.; Kang, B.-S.; Su, C.-Y. *Aust. J. Chem.* **2006**, *59*, 3.